



Entropy–Stabilized Metal Oxide Solid Solutions as CO Oxidation Catalysts with High–Temperature Stability

Journal:	<i>Journal of Materials Chemistry A</i>
Manuscript ID	TA-COM-02-2018-001772.R1
Article Type:	Communication
Date Submitted by the Author:	05-May-2018
Complete List of Authors:	Chen, Hao; The University of Tennessee, Department of Chemistry Fu, Jie; Zhejiang University, Department of Chemical and Biological Engineering Zhang, Pengfei; The University of Tennessee, Department of Chemistry Peng, Honggen; Nanchang University, Department of Chemistry Abney, Carter; Oak Ridge National Laboratory, Chemical Sciences Division Jie, Kecheng; The University of Tennessee, Department of Chemistry Liu, Xiaoming; Oak Ridge National Laboratory Chi, Miaofang; Oak Ridge National Laboratory, Center for Nanophase Materials Sciences Dai, Sheng; Oak Ridge National Laboratory,



Journal Name

COMMUNICATION

Entropy–Stabilized Metal Oxide Solid Solutions as CO Oxidation Catalysts with High–Temperature Stability

Received 00th January 20xx,
Accepted 00th January 20xx

Hao Chen^{a,c}, Jie Fu^c, Pengfei Zhang^a, Honggen Peng^{d,e}, Carter W. Abney^b, Kecheng Jie^a, Xiaoming Liu^d, Miaofang Chi^d, Sheng Dai^{a,b*}

DOI: 10.1039/x0xx00000x

www.rsc.org/

This work report a new strategy toward design of a new class of supported catalysts with intrinsic high–temperature stabilities through entropy maximization. The use of Pt, Ni, Mg, Cu, Zn, and Co not only enables the active sites to be highly dispersed for high catalytic activity in CO oxidation, but also results in extreme thermal stability (900 °C) owing to the entropy–stabilized behavior inside the metal oxide to survive the harsh conditions.

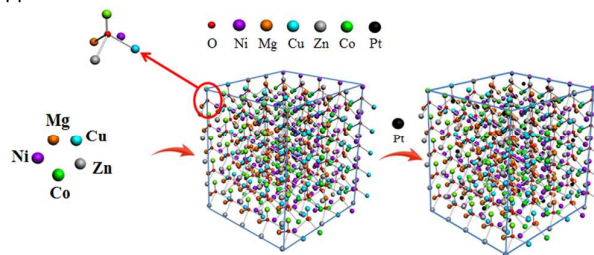
Supported metal catalysts play an essential role throughout chemical industries and environmental mitigations (e.g., steam reforming to produce H₂, automotive exhaust cleaning, activation of N₂ and CH₄).^{1–5} A major challenge in the design of efficient metal catalysts is overcoming the cohesive energy that drives co–domain formation and sintering at elevated temperatures. This difficulty is particularly acute in the design of supported catalyst systems, especially those possessing small quantities of homogeneously dispersed precious group metals.^{6–8} Due to their relatively low Tamman temperature⁹—the point at which supported metal crystallites develop liquid–like properties and exhibit an enhanced ability migrate¹⁰—sintering occurs rapidly, minimizing the surface area accessible for catalysis with commensurate reduction in activity.

Accordingly, significant effort has been devoted to designing functional catalyst systems which stabilize noble metal single atoms and nanoparticles at high temperature. For example, Joo and colleagues¹¹ reported Pt nanoparticles encaged in silica shells (Pt@mSiO₂) for ethylene hydrogenation and CO oxidation. Tian et al.¹² designed a heterostructured perovskite support for Au,

displaying high activity for CO oxidation and promising sintering resistance up to 750 °C. Arnal and coworkers¹ synthesized an Au based catalyst encapsulated in ZrO₂ hollow spheres. Following a 900 °C treatment, 100% CO conversion was achieved at 260–280 °C.

Recent work articulates the straightforward preparation of configurationally disordered and entropy–stabilized mixed metal oxides generated from earth–abundant materials.^{13–14} The isoivalent ensemble of binary oxide precursors are selected to ensure disparate crystal structure, electronegativity, and cation coordination geometry, resulting in formation of a single–phase rocksalt structure upon equilibration above 850 °C. Critically, complementary experiments definitively proved entropy to be the predominant force, affording a fully randomized final solid solution state. As the entropic contributions to Gibbs free energy are temperature dependent, we surmised introduction of noble metals into an appropriate mixed metal oxide solid solution would afford a randomly dispersed, homogeneous system of single atoms which are entropically stabilized at elevated temperatures and course function as an exciting new high–temperature catalyst.

In this work, we report the successful preparation of an entropy–stabilized, single–phase, mixed oxide (NiMgCuZnCoO_x) supported Pt high–temperature catalyst as shown in **Scheme 1**. The single–phase and entropically–driven stability of the PtNiMgCuZnCoO_x (0.3wt% Pt) endowed the catalyst with a superior activity for CO oxidation, even after treatment at 900 °C. We expect this exciting new synthetic approach will hold great promise for development of stabilized single atom materials for diverse applications.



Scheme 1. Scheme of the formation of 0.3wt%PtNiMgCuZnCoO_x entropy–stabilized metal oxide solid solution.

a Department of Chemistry, The University of Tennessee, Knoxville, TN, 37996, USA. E-mail: dais@ornl.gov.

b Oak Ridge National Laboratory, Oak Ridge, TN 37831, USA.

c Key Laboratory of Biomass Chemical Engineering of Ministry of Education, College of Chemical and Biological Engineering, Zhejiang University, Hangzhou, 310027, China.

d Center for Nanophase Materials Sciences, Oak Ridge National Laboratory, Oak Ridge, TN, 37831, USA.

e College of Chemistry, Nanchang University, 999 Xuefu Road, Nanchang, Jiangxi 330031, China

Electronic Supplementary Information (ESI) available: [details of any supplementary information available should be included here]. See DOI: 10.1039/x0xx00000x

Initially, the calcination temperatures of NiMgCuZnCoO_x were investigated at 800, 900, and 1000 °C to obtain the single entropy-stabilized phase. X-ray diffraction (XRD) patterns showing the phase evolution are depicted in Figure 1a. The five oxides were completely converted to a single phase when the calcination temperature was higher than 900 °C and there was no additional peak. Five peaks attributed to the (111), (200), (220), (311), and (222) planes of the entropy-stabilized oxide NiMgCuZnCoO_x were observed. From XRD shown in this and reported work^{13,15}, we knew that the NiMgCuZnCoO_x exhibited cubic rocksalt structure. Multiphases, rock salt, tenorite, and other crystal structures were observed in the sample calcinated at 800 °C^{13,15}. The entropy-stabilized phase can be formed at the calcination temperature higher than 900 °C. The TPR results (Figure S1) showed that the five metals formed the single phase and only one reduced peak for NiMgCuZnCoO_x and 0.3wt%PtNiMgCuZnCoO_x was detected. However, the total BET surface area (*S*_{BET}) for the sample calcinated at 900 °C was only 2 m²/g, probably due to the restructuring and growth of the crystalline phase. Then we used co-precipitation with cetyltrimethyl ammonium bromide and ammonium hydroxide to improve the synthesis method, and obtained an SBET of 28 m²/g for the entropy-stabilized metal oxide, which also exhibited a single phase in Figure 1b.

The catalytic oxidation of CO to CO₂ is one of the most widely studied surface reactions, and the catalysts reported were roughly of two types: noble metal based (Pt, Pd, Au)^{16–18} and metal oxide based (Cu, Co, Ce)^{19–21}. We then evaluated the catalytic activity for the oxidation of CO over the entropy-stabilized metal oxide in fixed-bed reactor at different temperature, which not only represents the activity of active sites, but also means the high-temperature stability for this material owing to its significance for pollution control and fuel cells²². As seen in Figure 1c, within a retention reaction time of less than 1 s, a CO conversion of 50% was achieved at 256 °C, and the complete conversion was achieved at 305 °C over both the catalysts calcinated at 900 °C by physical mixture and co-precipitation method. The catalyst calcinated at 1000 °C exhibited worse activity than those calcinated at 900 °C, and the conversions were 60% at 300 °C and 89% at 400 °C, respectively. We also evaluated the catalytic activities over the catalysts including NiCuZnCoO_x (mix), NiMgCuCoO_x (mix), NiMgZnCo (mix), NiMgCuZnO_x (mix) and MgCuZnCo (mix) indicating that this single entropy-stabilized phase might be destroyed when individual components were removed¹³.

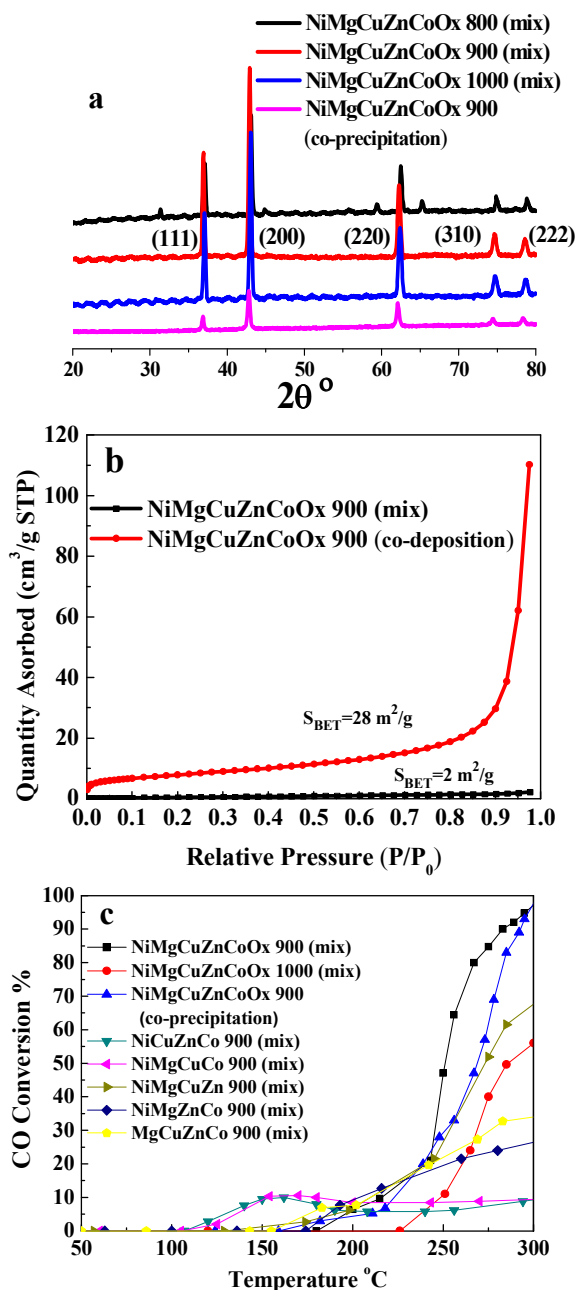


Figure 1. (a) X-ray diffraction patterns for NiMgCuZnCoO_x; (b) Nitrogen adsorption-desorption isotherms of NiMgCuZnCoO_x synthesized by physical mixture and co-precipitation method. (c) CO oxidation activity of NiMgCuZnCoO_x synthesized by physical mixture and co-precipitation method. Reaction condition: a catalyst loading of 20 mg, a flow rate of 12.5 mL/min, and 1 vol % CO balance in air.

Although NiMgCuZnCoO_x exhibited considerable activity for the CO oxidation, there is a need for the conversion of CO in low temperature. Pt was known for the high activity for CO oxidation, and it was introduced into the catalyst to form entropy-stabilized metal oxide solid solution. After the introduction of Pt during the synthesis, only five peaks attributed to the entropy-stabilized oxide

were observed both for as-synthesized and reduced PtNiMgCuZnCoO_x without the Pt peak, shown in the XRD results in **Figure 2**. The particles are large and thick due to the high-temperature calcination. The lack of a Pt or PtO_x peak suggests the Pt atoms were highly dispersed in the entropy-stabilized oxide, and no sintering of Pt occurred even after calcinated at 900 °C. The entropy-stabilized oxide was maintained, and no Pt atom was aggregated after the H₂ reduction at 300 °C for 2 h.

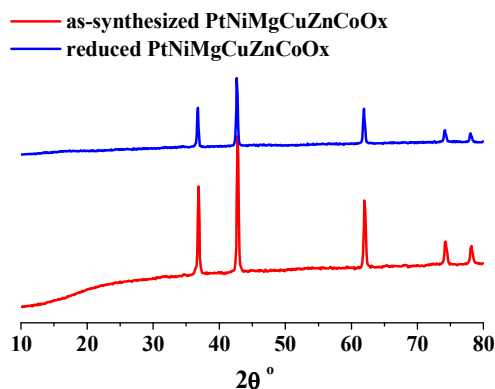


Figure 2. X-ray diffraction patterns for as-synthesized and reduced 0.3wt%PtNiMgCuZnCoO_x synthesized by co-precipitation.

Further characterizations of the single phase were conducted using high resolution transmission electron microscopy (HRTEM), high-angle annular dark-field scanning transmission electron microscopy (HAADF-STEM) and energy-dispersive x-ray spectroscopy (EDS) to determine the crystal lattice and elementary composition of the entropy-stabilized metal oxide solution. The results are shown in **Figures 3 and S2~3**. The particles are large and thick as shown in **Figure S2** due to the high temperature treatment. The EDS signals for the K α emission energies of Ni, Mg, Cu, Zn, and Co in **Figure S3** suggest that all the magnifications revealed a chemically and structurally homogeneous material, and the areal distribution of colors was random and free from clustering. In **Figure 3**, the TEM and HAADF-STEM images of reduced 0.3wt%PtNiMgCuZnCoO_x shows that the crystal lattice was single, meaning that the Pt atoms were dissolved into the entropy-stabilized metal oxide. Thus, it can be concluded that the cations were uniformly dispersed. As shown in **Figure 3**, marked atoms might be the Pt single atom as they were slightly brighter than the surrounding atoms. Corresponding intensity profiles can be seen, and the dashed boxes shown in image indicate locations where the intensity profiles were obtained. An obvious intensity increase close to the surface indicates the existence of the Pt single atom.

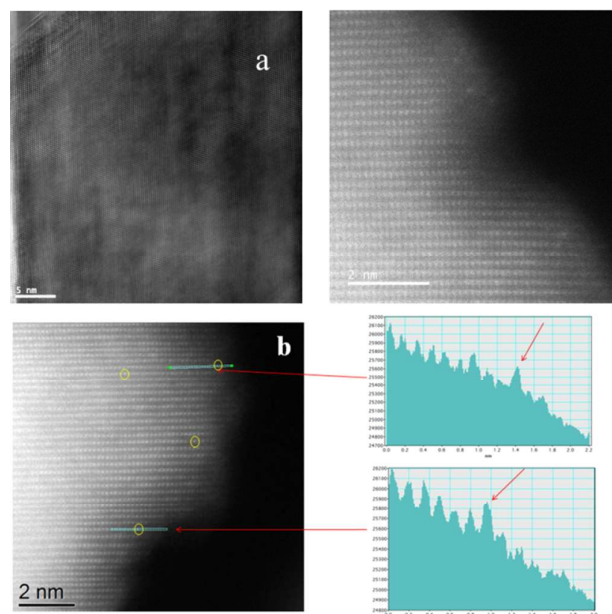


Figure 3. TEM and HAADF-STEM images of reduced 0.3wt%PtNiMgCuZnCoO_x.

Subsequently, the low-temperature catalytic activities of the as-synthesized and reduced 0.3wt%PtNiMgCuZnCoO_x samples for CO oxidation were evaluated. As shown in **Figure 4**, the 0.3wt%PtNiMgCuZnCoO_x sample exhibited much better activity for the oxidation of CO compared to the NiMgCuZnCoO_x sample. The reduced 0.3wt%PtNiMgCuZnCoO_x sample became active at 60 °C. The CO was completely converted at 155 °C over the reduced 0.3wt%PtNiMgCuZnCoO_x and at 245 °C over the as-synthesized 0.3wt%PtNiMgCuZnCoO_x, both lower than the temperature of complete conversion over NiMgCuZnCoO_x (305 °C), indicating that the Pt and PtO_x played an important role in the CO oxidation. Several Pt single atom-based catalysts have been recently reported for the oxidation of CO to CO₂^{23, 24} and the atomically dispersed ionic Pt²⁺²⁴ is usually considered as the active site for the CO oxidation because the Pt⁰ has an inhibiting effect on CO oxidation at low temperatures due to the competitive adsorption between Pt⁰ and CO. It was also reported that thermal treatment at high temperature led to strong Pt–O–M bond formation.²⁴ Thus, we proposed that the Pt atom in this work existed as Pt–O–M or O–Pt–O–M (M: Ni, Mg, Cu, Zn, Co) atomically dispersed Pt. The reduction by H₂ was to reduce the O–Pt–O–M (Pt⁴⁺) to Pt–O–M (Pt²⁺) and improve the activity of catalyst. The main active site was Pt²⁺ (Pt–O–M) in 0.3wt%PtNiMgCuZnCoO_x entropy-stabilized oxide, and a part of Pt atoms formed Pt–O phase. Survey scans of the reduced 0.3wt%PtNiMgCuZnCoO_x by X-ray photoelectron spectroscopy (XPS) are shown in **Figure S4**. There is no evidence of Pt related signals for the Pt 4d, Pt 4f or Pt 3p_{3/2}, possible due to the formation of Pt-based NiMgCuZnCo metal oxide solid solutions with Pt species staying in the bulk. The reduced 0.3wt%PtNiMgCuZnCoO_x showed high stability during the catalytic oxidation of CO to CO₂ at 135 °C for at least 40 h reaction time without loss of its catalytic activity.

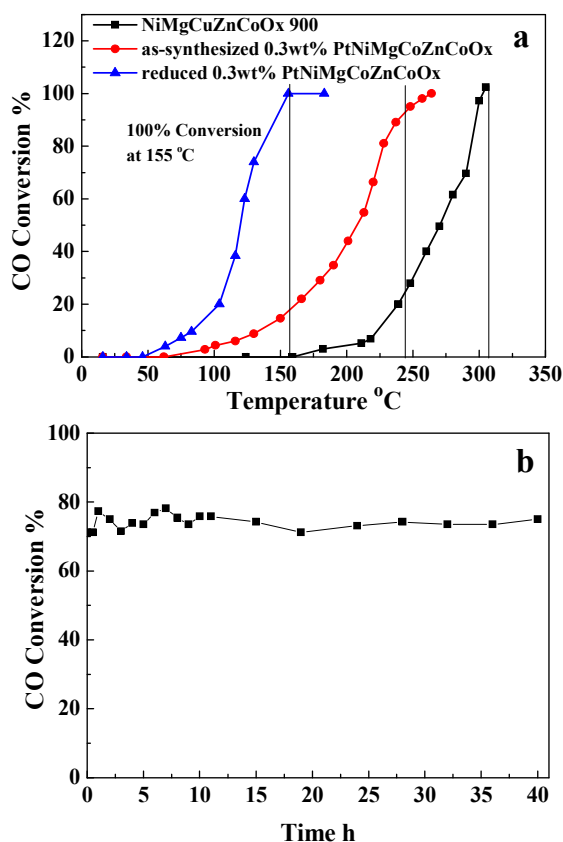


Figure 4. (a) CO oxidation activity of 0.3wt%PtNiMgCuZnCoO_x synthesized by co-precipitation. (b) CO oxidation activity of reduced 0.3wt%PtNiMgCuZnCoO_x synthesized by co-precipitation upon reaction time under reaction temperature of 135 °C. Reaction condition: a catalyst loading of 20 mg, a flow rate of 12.5 mL/min, and 1 vol % CO balance in air.

The reaction rate constants (k) and apparent activation energy (E_a) were calculated according to CO conversions at different temperatures over NiMgCuZnCoO_x, as-synthesized 0.3wt%PtNiMgCuZnCoO_x, and reduced 0.3wt%PtNiMgCuZnCoO_x. The calculation method and experimental data were shown in [Figure S7](#) and [Table S1](#). The calculated E_a of CO oxidation over NiMgCuZnCoO_x 900 (211~299 °C), as-synthesized 0.3wt%PtNiMgCuZnCoO_x (160~237 °C), and reduced 0.3wt%PtNiMgCuZnCoO_x (63~136 °C) were 91.5, 57.2 and 54.8 kJ mol⁻¹, respectively. Thus, the low E_a indicates that the atomically dispersed Pt in 0.3wt%PtNiMgCuZnCoO_x was indeed active for CO oxidation and significantly enhanced the low-temperature activity of CO oxidation by decreasing the reaction barrier.²⁵

Maintaining high activity and surviving the harsh conditions are very important for the industrial catalysis. In this work, we introduce the concept of an entropy-stabilized phase, which dominates the thermodynamic landscape by formulating an oxide with five or more components. This homogeneous metal solid solution of five binary oxides not only exhibited high stability but also acted as a promising support for Pt to form an efficient catalyst for the oxidation of CO.

Conclusions

In summary, a simple, low-cost, and easy-magnifying synthesis approach for entropy-stabilized metal oxide solid solutions were developed. The synthesized entropy-stabilized metal oxide solid solution NiMgCuZnCoO_x can act both as a CO oxidation catalyst and as an excellent support to stabilize highly dispersed even single atomically dispersed platinum species, even at temperatures up to 900 °C. The use of Pt, Ni, Mg, Cu, Zn, and Co not only enables the active sites to be highly dispersed for high catalytic activity in CO oxidation but also results in extreme thermal stability owing to the entropy-stabilized behavior inside the metal oxide solution to survive the harsh conditions. The catalyst showed good reusability for at least 40 h without any reduction in the catalytic activity.

Conflicts of interest

There are no conflicts to declare.

ACKNOWLEDGMENT

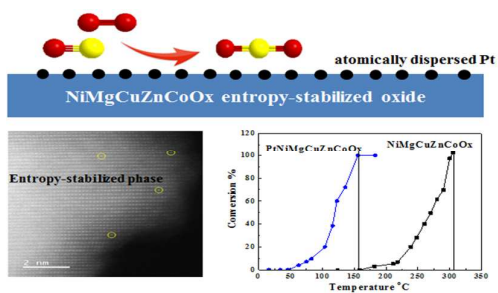
SD was supported by the Division of Chemical Sciences, Geosciences, and Biosciences, Office of Basic Energy Sciences, US Department of Energy. Electron microscopy work was supported by the U.S. DOE, Office of Science, Basic Energy Sciences, Materials Sciences and Engineering Division (MC, XL), and was conducted at the Center for Nanophase Materials Sciences, which is a DOE Office of Science User Facility operated by the Oak Ridge National Laboratory.

Notes and references

- 1 P. M. Arnal, M. Comotti and F. Schüth, *Angew. Chem. Int. Ed.*, 2006, **118**, 8404–8407.
- 2 A. T. Bell, *Science*, 2003, **299**, 1688–1691.
- 3 C. Chen, C. Nan, D. Wang, Q. Su, H. Duan, X. Liu, L. Zhang, D. Chu, W. Song, Q. Peng and Y. Li, *Angew. Chem. Int. Ed.*, 2011, **50**, 3725–3729.
- 4 H. Tang, J. Wei, F. Liu, B. Qiao, X. Pan, L. Li, J. Liu, J. Wang and T. Zhang, *J. Am. Chem. Soc.*, 2016, **138**, 56–59.
- 5 K. An, S. Alayoglu, N. Musselwhite, K. Na and G. A. Somorjai, *J. Am. Chem. Soc.*, 2014, **136**, 6830–6833.
- 6 J. Jones, H. Xiong, A. T. DeLaRiva, E. J. Peterson, H. Pham, S. R. Challa, G. Qi, S. Oh, M. H. Wiebenga, X. I. P. Hernández, Y. Wang and A. K. Datye, *Science*, 2016, **353**, 150–154.
- 7 E. J. Peterson, A. T. DeLaRiva, S. Lin, R. S. Johnson, H. Guo, J. T. Miller, J. H. Kwak, C. H. Peden, B. Kiefer and L. F. Allard, *Nat. Commun.*, 2014, **5**, 4885.
- 8 H. Yan, H. Cheng, H. Yi, Y. Lin, T. Yao, C. Wang, J. Li, S. Wei and J. Lu, *J. Am. Chem. Soc.*, 2015, **137**, 10484–10487.
- 9 G. Tammann, *Lehrbuch der Metallkunde*, 4. Ed., Verlag Voss, Berlin 1929.
- 10 C. H. Bartholomew, *Appl. Catal. A: Gen.*, 2001, **212**, 17–60.
- 11 S. H. Joo, J. Y. Park, C. K. Tsung, Y. Yamada, P. Yang and G. A. Somorjai, *Nat. Mater.*, 2009, **8**, 126–131.
- 12 C. Tian, X. Zhu, C. W. Abney, X. Liu, G. S. Foo, Z. Wu, M. Li, H. M. Meyer, S. Brown, S. M. Mahurin, S. Wu, S. Z. Yang, J. Liu and S. Dai, *ACS Catal.*, 2017, **7**, 3388–3393.

- 13 C. M. Rost, E. Sachet, T. Borman, A. Moballegh, E. C. Dickey, D. Hou, J. L. Jones, S. Curtarolo and J. P. Maria, *Nat. Commun.*, 2015, **6**, 8485.
- 14 A. Sarkar, R. Djenadic, N. J. Usharani, K. P. Sanghvi, V. S. K. Chakravadhanula, A. S. Gandhi, H. Hahn and S. S. Bhattacharya, *J. Eur. Ceram. Soc.*, 2017, **37**, 747–754.
- 15 C. M. Rost, Z. Rak, D. W. Brenner and J. P. Maria, *J. Am. Ceram. Soc.*, 2017, **100**, 2732–2738.
- 16 R. D. Monte, P. Fornasiero, J. Kašpar, P. Rumori, G. Gubitto and M. Graziani, *Appl. Catal. B: Environ.*, 2000, **24**, 157–167.
- 17 Z. Y. Li, Z. Yuan, X. N. Li, Y. X. Zhao and S. G. He, *J. Am. Chem. Soc.*, 2014, **136**, 14307–14313.
- 18 M. Moses–DeBusk, M. Yoon, L. F. Allard, D. R. Mullins, Z. Wu, X. Yang, G. Veith, G. M. Stocks and C. K. Narula, *J. Am. Chem. Soc.*, 2013, **135**, 12634–12645.
- 19 Z. G. Liu, S. H. Chai, A. Binder, Y. Y. Li, L. T. Ji and S. Dai, *Appl. Catal. A: Gen.*, 2013, **451**, 282–288.
- 20 V. Choudhary, K. Mondal and A. Mamman, *J. Catal.*, 2005, **233**, 36–40.
- 21 X. Xie, Y. Li, Z. Q. Liu, M. Haruta and W. Shen, *Nature*, 2009, **458**, 746–749.
- 22 J. A. Rodriguez, D. C. Grinter, Z. Liu, R. M. Palomino and S. D. Senanayake, *Chem. Soc. Rev.*, 2017, **46**, 1824–1841.
- 23 B. Qiao, A. Wang, X. Yang, L. F. Allard, Z. Jiang, Y. Cui, J. Liu, J. Li and T. Zhang, *Nat. Chem.*, 2011, **3**, 634–641.
- 24 L. Nie, D. Mei, H. Xiong, B. Peng, Z. Ren, X. I. P. Hernandez, A. DeLaRiva, M. Wang, M. H. Engelhard, L. Kovarik, A. K. Datye, and Y. Wang, *Science*, 2017, **358**, 1419–1423.
- 25 S. Yao, X. Zhang, W. Zhou, R. Gao, W. Xu, Y. Ye, L. Lin, X. Wen, P. Liu, B. Chen, E. Crumlin, J. Guo, Z. Zuo, W. Li, J. Xie, L. Lu, C. J. Kiely, L. Gu, C. Shi, J. A. Rodriguez, and D. Ma, *Science*, 2017, **357**, 389–393.

TOC Graphic:



Entropy-Stabilized Metal Oxide Solid Solutions as CO Oxidation Catalysts with High-Temperature Stability.